A Study on Passenger Flow Control Scheme for Single-line Multi-station Urban Mass Transit Considering Passenger Flow Loss

Lizhong Zhu, Xinfeng Yang and Xianglong Huo

Abstract—**The volume of inbound passenger flow at urban rail stations during peak hours is often excessive, which poses potential safety hazards to passengers. In addition, it also reduces the fairness of passenger services at the various stations and leads to inconvenience in the operation of these stations. Therefore, a nonlinear multi-objective planning model with the constraints of the maximum passenger density in the waiting area, the maximum section carrying capacity, and the passenger flow control coefficients are established to find the optimal flow control scheme. The model aims to minimize the variance of the average passenger dwell time and the count of lost passengers at all stations of the line. A hybrid simulated annealing particle swarm optimization algorithm (SA-PSO) is designed to solve the model. The up direction of Shenzhen Urban Mass Transit Line 4 is adopted here as an example for research. The research results indicate that the optimal passenger flow control scheme can effectively reduce the sum of lost passengers and maintain passenger density within the safety range in all waiting areas at each station. Additionally, it is observed that under the optimal passenger flow control scheme, the average dwell time of all stations is more balanced. Overall, the optimized flow control scheme is more effective in coping with large urban rail passenger flows than several no flow control and non-optimized flow control schemes.**

Index Terms—**urban rail transport, passenger flow control, peak hours, lost passengers, average passenger dwell time**

I. INTRODUCTION

DUE to urbanization and dense population, managing heavy passenger flows is a constant challenge for urban mass transit systems. During peak hours, some popular stations experience overcrowded passenger flow due to an imbalance in the spatial distribution of passenger flow. This phenomenon creates a significant contradiction between the demand for passenger flow and the uneven distribution of transportation resources. Therefore, resolving the issue of ensuring safety and maximizing the effectiveness of urban mass transit while managing large passenger volumes is a significant challenge.

In terms of considering safety, Jungang Shi et al.[1] proposed a method to mitigate the risk of passenger flow aggregation and enhance passenger safety. The method serves two purposes: reducing the risk of passenger flow aggregation and shortening the waiting time of passengers. Zhiya Chen et al.[2] developed a three-level passenger flow control model by managing passenger flow at both line and station levels. The model aims to tackle security and congestion issues during peak hours in different regions. Jungang Shi et al.[3] assume that passengers can transfer trains across multiple urban rail transit lines with just one ticket. Their model aims to reduce passenger waiting time and minimize the risk of congestion at all relevant stations.

In terms of considering controlling strength, Denghui Li et al.[4] established a model to calculate the flow control rate of each station. In order to determine the flow control intensity of the station. Peng Zhao et al.[5] built a coordinated control model between stations and time segments at the line level by using mathematical planning techniques. Meanwhile, they also used the solved flow control rate as a quantitative basis for implementing flow-limiting measures.

In terms of combining passenger flow control with train scheduling schemes, Bin Jia et al.[6] evaluated various random scenarios to understand the uncertainty surrounding passenger arrival rates. They integrated the passenger arrival rates, mixing long and short running routes, passenger flow control schemes, and dynamic departure intervals for collaborative optimization of train schedules. Housheng Zhou et al.[7] developed a two-stage stochastic programming model in order to optimize the flexible marshalling mode train utilization plan and robust passenger flow control scheme collaboratively. From the perspective of the entire urban mass transit system, Yahan Lu et al.[8]'s research examined the coupling relationship between train flow and passenger flow. And they built a model to optimize the train timetable and passenger flow control. Fuya Yuan et al.[9] considered the impact of station entrances, platforms, and train capacity on the count of passengers getting on and off in a flexible station hopping mode. Jiajie Li et al.[10] suggested a combined optimization of inbound passenger control and train service planning. It can solve the suburban urban rail lines' oversaturation issue. A synergistic optimization model of outside station flow restriction and train arrival and

Manuscript received July 10, 2023; revised November 27, 2023.

This work was supported in part by Double-First Class Major Research Programs, Educational Department of Gansu Province (No. GSSYLXM-04), Projects Funded by the Central Government to Guide Local Scientific and Technological Development (No. 22ZY1QA005), Young Scientists Fund of School of Traffic and Transportation, Lanzhou Jiaotong University (No. YQN202204).

Lizhong Zhu is a postgraduate student at School of Traffic and Transportation, Lanzhou Jiaotong University, Lanzhou 730070, China. (e-mail: 17339901027@163.com).

Xinfeng Yang is a professor at School of Traffic and Transportation, Lanzhou Jiaotong University, Lanzhou 730070, China; he is a professor at Key Laboratory of Railway Industry on Plateau Railway Transportation Intelligent Management and Control, Lanzhou Jiaotong University, Lanzhou 730070, China. (Corresponding author, e-mail: xinfengyang@mail.lzjtu.cn).

Xianglong Huo is a ROT of Trainee, MTR Corporation (Shenzhen) Limited, ShenZhen 518109, China. (e-mail:xlhuo@mtrsz.com.cn).

departure moments in the event of high passenger flow at urban rail transit interchange stations was developed by Jiajie Li et al.[11].

Regarding passenger flow control errors, Xiangming Yao et al.[12] developed a robust optimization model. The model aims to minimize the sum of passenger delay time outside the station and maximize passenger turnover. Jinpeng Liang et al.[13] developed an online control scheme aiming to manage the influx of passengers for each OD pair efficiently. This plan aims to reduce the sum of passenger waiting time in urban rail lines.

In terms of considering passenger flow demand, Yahan Lu et al.[14] constructed an optimization model for passenger flow control schemes and train schedules. The model is based on the uncertainty of passenger flow at each station. Qiwei Jiang et al.[15] constructed a synchronous optimization model for multi-station passenger flow control. The model considers the time-varying and uneven passenger flow demand characteristics.

The station's three-level passenger flow control scheme is the basis of this paper. The relationship between urban rail single-line and station passenger flow control has also been fully considered. On the basis of analyzing the influencing factors of passenger flow loss, a collaborative optimization model of multi-station passenger flow control with careful consideration of safety and fairness is proposed. Most of the researchers have only examined the passenger flow control schemes for arrivals at a single station or a single urban rail line without considering the possibilities of merging station and line passenger flow control. Besides, the results of these studies usually assume that long detention times don't cause passengers to abandon taking urban mass transit. Therefore, the optimization model aims to minimize passenger flow loss, ensure passenger safety and efficiently allocate transportation capacity by coordinating the flow at each station over time.

This paper is organized as follows: Section II presents the problem, Section III describes the mathematical model design, Section IV presents the proposed algorithm design, Section V analyzes the model with examples, and finally, the conclusion is provided.

II. Description of The Problem

Urban rail transit often experiences heavy passenger flow during the morning rush hour, which tends to result in a congregation of passengers. This presents a safety risk as the total transportation demand exceeds the carrying capacity, leaving many passengers stranded inside and outside the station. Moreover, although trains running to the upstream stations have sufficient capacity, the limited capacity of trains running to the middle and downstream stations often forces some passengers to stay at the station platform. In order to ensure a balanced service for passengers during peak hours, it is crucial to implement passenger flow control at each station on urban rail lines.

In this paper, the term "flow control" has two meanings. Firstly, it involves regulating the count of passengers in the waiting area outside the station, in the station concourse, and on the platform. The primary purpose is to ensure the safety of passengers in different station areas. Meanwhile, the different schemes for controlling passenger flow in paid and non-paid areas at the station concourse level will not be addressed. Secondly, flow control also aims to equalize the count of passengers at each station of the line to ensure fairness of service. Passenger congestion typically occurs in one direction during weekday peak hours. Therefore, one of the typical unidirectional urban rail lines with stations numbered 1 to S in the direction of train operation is chosen as the object of study, as shown in Fig. 1.

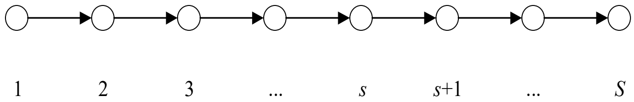

Fig. 1. One-way route map for urban rail

III. Model Construction

A. Model assumptions and parameter definitions

There are some following assumptions to simplify the analysis in this paper:

(1) The transport capacity of the zone is known, and trains adhere to defined operating charts.

(2) Exclude cases where passengers willingly choose to remain and wait for the following train.

(3) The passenger flow status remains stable and evenly distributed during the control period.

(4) Simplify the process of entering and exiting the station for passengers. Passenger walking time within the station is not in view and does not consider the occupancy of the platform by outbound passengers and their interference with inbound passengers walking.

To convey the issue more precisely, Table I provides the descriptions of the model parameters.

TABLE I
PARAMETERS AND VARIABLES IN THE PROPOSED MODEL

Parameters	Definition
s	Sequential numbering of stations on the line in one direction, s=1,2,3, ..., S
t	Numbering of the restricted periods, t=1,2,3, ..., T
Δt	Duration of passenger flow control periods
$C_s^u(t)$	Number of new arrivals at station s at stage t
C	Train capacity
σ_{max}	Maximum full train load factor
ρ	Maximum safe passenger flow density in passenger waiting areas
θ	Churn rate
S_j	Effective area of passenger waiting area, j=1,2,3 indicates that passengers are located outside the station, in the station concourse, and on the platform, respectively
Intermediate variable	Definition
$C_s^r(t)$	Actual passenger flow at station s at stage t
$C_s^{h_3}(t)$	Number of stranded passengers outside the station s at the end of the stage t
$C_s^{w_3}(t)$	Number of outside station passengers lost due to hold-up at station s at stage t
$C_s^{h_2}(t)$	Number of stranded passengers in the station s concourse at the end of the stage t
$C_s^{w_2}(t)$	Number of passengers in station s lost to detention in the station concourse at stage t
$C_s^b(t)$	Actual number of passengers waiting in the station s concourse at stage t
$C_s^{dn}(t)$	Number of alighting passengers at station s at stage t

$C_s^p(t)$	Number of boarding passengers permitted at station s at stage t
$C_s^d(t)$	Number of passengers waiting on the platform of the station s at stage t
$C_s^{h_1}(t)$	Number of stranded passengers on the platform of the station s at the end of the stage t
$C_s^{w_1}(t)$	Number of passengers lost on the platform due to hold-up at station s at stage t
$q_s^{on}(t)$	Passenger flow between station s to station s+1 at stage t
$E_s(t)$	Passenger dwell time at station s at stage t
$C_s^{\max}(t)$	Maximum section carrying capacity between station s to station s+1 at stage t
$n_s(t)$	Number of trains passing between station s to station s+1 at stage t
η_s	Alighting rate at station s
μ_j	Time perception coefficients, j=1,2,3 indicate that the passenger is located outside the station, in the station concourse, and on the platform, respectively
$M_j^s(t)$	Passenger crowding in the passenger waiting area of station s at stage t, j=1,2,3 indicates that passengers are located on the platform, in the station concourse, and outside the station, respectively
Decision variable	Definition
$x_s(t)$	Number of passengers permitted to enter the station at station s at stage t
$y_s(t)$	Number of passengers permitted to enter the platform at station s at stage t

B. Decision variables, constraints and functions

The decision variables included in this model are all integer variables: the number of passengers permitted to enter the station ($x_s(t)$) and the number of passengers allowed into the platform ($y_s(t)$). All other variables are non-negative.

(1) Outside station passenger flow constraints

During each control period, the waiting passenger flow outside each station is composed of new arrivals and stranded passengers from the previous period. The count of stranded passengers is negatively correlated with the count of lost passengers outside the stations. The calculation of the outside station waiting passengers, stranded passengers, and lost passengers is shown in equations (1)-(4) below.

$$C_s^r(t)=\begin{cases} C_s^u(t), & t=1 \\ C_s^u(t)+C_s^{h_3}(t-1), & t=2,3,...,T \end{cases} \tag{1}$$

$$C_s^{h_3}(t)=C_s^r(t)-x_s(t)-C_s^{w_3}(t) \tag{2}$$

$$C_s^{w_3}(t)=\mu_3 M_3^s(t)(C_s^r(t)-x_s(t))\theta \tag{3}$$

$$0.5C_s^r(t)\le x_s(t)\le C_s^r(t) \tag{4}$$

Equation (1) represents the actual passenger flow for each period outside each station, including both newly arriving passengers and stranded passengers from the previous period outside the station. Equations (2) and (3) are utilized for calculating the outside station stranded passengers and lost passengers for each period. Equation (2) represents the stranded passenger flow outside the station ($C_s^{h_3}(t)$). The equation includes the actual passenger flow, permitted to enter the station passenger flow, and the lost passengers outside the station. Equation (3) represents the lost passenger flow outside the station ($C_s^{w_3}(t)$). This equation includes four factors: the count of passengers not permitted to enter the concourse, the passenger loss factor, the crowding factor, and the passenger time perception factor. Besides, equation (4) states that the count of passengers permitted to enter the station must be at least half of the actual passenger flow for each period outside each station. Meanwhile, it cannot exceed the actual passenger flow. In simpler terms, the flow control factor cannot exceed 0.5 [4].

(2) Station concourse passenger flow constraints

Equations (5)-(8) below calculate the actual passenger flow waiting to enter the platform at each station during the control period. The actual passenger flow is determined by the permitted to enter the platform passenger flow and the count of passengers stranded in the previous period. The count of stranded passengers is negatively correlated with the count of lost passengers in the concourse. Therefore, the actual number of passengers waiting to enter the platform at each station can be measured by the actual passenger flow, the count of stranded passengers, and the count of lost passengers in the concourse.

$$C_s^b(t)=\begin{cases} x_s(t), & t=1 \\ x_s(t)+C_s^{h_2}(t-1), & t=2,3,...,T \end{cases} \tag{5}$$

$$C_s^{h_2}(t)=C_s^b(t)-y_s(t)-C_s^{w_2}(t) \tag{6}$$

$$C_s^{w_2}(t)=\mu_2 M_2^s(t)(C_s^b(t)-y_s(t))\theta \tag{7}$$

$$0.5C_s^b(t)\le y_s(t)\le C_s^b(t) \tag{8}$$

Equation (5) represents the actual passenger flow in the concourse at each station for all periods. The flow includes both newly permitted to enter the station passengers and stranded passengers in the concourse during the previous period. Equations (6) and (7) provide the calculation for stranded and lost passengers in the concourse at all stations during each period. Equation (6) shows the stranded passengers in the concourse ($C_s^{h_2}(t)$). It includes the actual passenger flow, permitted to enter the platform passenger flow, and lost passenger flow in the concourse. Equation (7) determines the count of lost passengers in the concourse ($C_s^{w_2}(t)$) based on four factors: the count of passengers not permitted to enter the the platform, the passenger loss factor, the crowding factor, and the passenger time perception factor. Equation (8) states that the flow control factor cannot exceed 0.5 [4]. The equation implies that the count of passengers permitted to enter the platform must be at least 50% of the passenger flow in the station concourse. Meanwhile, it should be within the limits of the actual passenger flow in the station concourse.

(3) Station platform passenger flow constraints

For each control period, the actual waiting passenger flow on the platform of each station consists of the count of passengers stranded in the previous period and the count of permitted to board passengers. The count of stranded passengers is negatively correlated with the count of lost passengers on the platform. The calculation formulas for the actual passenger flow on the platform are shown in equations (9)-(12).

$$C_s^d(t)=\begin{cases} y_s(t), & t=1 \\ y_s(t)+C_s^{h_1}(t-1), & t=2,3,...,T \end{cases} \tag{9}$$

$$C_s^{h_1}(t)=C_s^d(t)-C_s^p(t)-C_s^{w_1}(t) \tag{10}$$

$$C_s^{w_1}(t)=\mu_1 M_1^s(t)(C_s^d(t)-C_s^p(t))\theta \tag{11}$$

$$\sum_{s=1}^{S} C_s^{h_1}(T)=0 \tag{12}$$

Equation (9) represents the actual passenger flow on the platform at all stations for each period, including both newly permitted to enter the platform passengers and stranded passengers during the previous period on the platform. Equation (10) shows the stranded passengers on the platform ($C_s^{h_1}(t)$). The equation includes the permitted boarding passenger flow, the actual passenger flow, and the lost passenger flow on the platform during each period. Besides, the count of lost passengers on the platform ($C_s^{w_1}(t)$) is shown in equation (11). The equation includes four factors: the passenger time perception factor, the crowding factor, the passenger loss factor, and the count of passengers not permitted to board. After the flow control T period, equation (12) states that the count of stranded passengers is zero on the platform at all stations. The equation aims to ensure that service is available to every passenger permitted to enter the platform at each station.

(4) Passenger boarding and alighting constraints

The passenger boarding and alighting demand includes the count of passengers getting off and boarding the vehicle. These quantities are determined using equations (13) and (14) provided below.

$$C_s^p(t) = \min\{C_s^{\max}(t) - q_{s-1}^{on}(t), C_s^d(t)\} \tag{13}$$

$$C_s^{dn}(t) = \begin{cases} 0, & s = 1 \\ \eta_s \cdot q_{s-1}^{on}(t), & s = 2,3,...,T \end{cases} \tag{14}$$

Equation (13) states that the count of permitted boarding passengers is determined by the lesser value between the remaining train capacity and the count of waiting passengers on the platform. Besides, the passenger alighting process is described in equation (14). If station s serves as the starting station, no one alights. However, if station s is not the starting station, the count of passengers alighting equals the product of the count of passengers carried by train at station s-1 and the alighting rate at station s.

(5) Section carrying capacity constraints

Equations (15)-(17) provide the maximum section carrying capacity expressions. The count of trains, train seating capacity, and maximum full load rate determine this capacity. These equations aim to limit the passenger flow passing through the section.

$$C_s^{\max}(t) = n_s(t) \cdot C \cdot \sigma_{\max} \tag{15}$$

$$q_s^{on}(t) = \begin{cases} C_s^p(t), & s = 1 \\ q_{s-1}^{on}(t) + C_s^p(t) - C_s^{dn}(t), & s = 2,3,...,T \end{cases} \tag{16}$$

$$q_s^{on}(t) \le C_s^{\max}(t) \tag{17}$$

Equation (15) shows that the maximum full load rate, the count of passing trains, and the train seating capacity during the flow control period determine the maximum section carrying capacity. Equation (16) states that if station s is the starting station, the passing passenger flow between stations s and s+1 equals the permitted boarding passenger flow at the starting station. On the other hand, if station s is not the starting station, the passing passenger flow between stations s and s+1 at stage t can be calculated by adding the count of passengers passing through the previous section with the boarding passengers at station s and subtracting the alighting passengers at station s. Furthermore, equation (17) emphasizes that the count of passengers passing between station s and station s+1 at stage t must not exceed the maximum section carrying capacity during the flow control period.

(6) Maximum safe passenger density constraints

In order to minimize safety hazards caused by passenger accumulation in each waiting area, the maximum safe passenger density is designed. This density is defined by equations (18)-(20) below.

$$\frac{C_s^r(t)}{S_3} \le \rho \tag{18}$$

$$\frac{C_s^b(t)}{S_2} \le \rho \tag{19}$$

$$\frac{C_s^d(t)}{S_1} \le \rho \tag{20}$$

Equations (18)-(20) show that passenger density in various waiting areas, including outside the station, concourse, and platform, must not exceed the maximum safe limit.

(7) Crowding function

The passenger aggregation risk in waiting areas at different stations is classified into five levels based on the queuing area service levels listed in Table II[16] and the density of stranded passengers. The value of the crowding degree increases as the passenger density level increases. To provide a more visual representation of passenger aggregation risk, thresholds for passenger density levels are represented by variables m_1~m_4. These variables are defined as follows: m_1 = 0.83p/m^2, m_2 = 1.11p/m^2, m_3 = 1.43p/m^2, and m_4 = 3.33p/m^2. This crowding degree serves as the basis for constructing the crowding degree function shown in equation (21) below.

$$M_j^s(t) = \begin{cases} 0.5, & F_j / S_j \le m_1 \\ 0.75, & m_1 < F_j / S_j \le m_2 \\ 1, & m_2 < F_j / S_j \le m_3 \\ 1.25, & m_3 < F_j / S_j \le m_4 \\ 1.5, & m_4 < F_j / S_j \le \rho \end{cases} \tag{21}$$

TABLE II
DESCRIPTION OF THE HIERARCHY OF SERVICE LEVELS IN THE QUEUING AREA

Service Level	Number of standing people per unit area (p/m²)	Grading Description
A	<0.83	Free to stand and move around
B	0.83~1.11	Activities carried out are partially restricted by avoidance of others
C	1.11~1.43	Standing and movement will be limited, but the passenger density is within a comfortable range
D	1.43~3.33	Mobility is greatly restricted and contact with others is unavoidable when standing
E	>3.33	Inevitable contact with others, inability to move, resulting in severe discomfort

Equation (21) represents the congestion level in waiting areas at station s during the control period t. Fj represents the count of passengers in each waiting area, where j=1,2,3 denotes passengers outside the station, in the concourse, and on the platform, respectively.

C. Objective function

There are primarily focuses on two passenger-oriented aspects in this paper: minimizing the ratio of lost passenger flow to arriving passenger flow, and reducing the variance of average passenger dwell time during the morning peak hours on the line.

(1) Minimize the percentage of total lost passenger flow

Equation (22) shows the ratio of lost passengers to arrivals. The lost passengers include those in various waiting areas during the flow control period at all stations.

$$\min Z_1 = \frac{\sum_{s=1}^{S}\sum_{t=1}^{T}\sum_{j=1}^{3} C_s^{w_j}(t)}{\sum_{s=1}^{S}\sum_{t=1}^{T} C_s^{u}(t)} \tag{22}$$

(2) Minimizing the variance of the average passenger dwell time

Equation (23) describes the calculation of total passenger dwell time at each station for each period. The time perception coefficients of different waiting areas and the actual passenger dwell time combine to form the passenger dwell time. Besides, the variance expression of the average passenger dwell time at all stations during the control period is shown in equation (24).

$$E_s(t) = \sum_{j=1}^{3} C_s^{h_j}(t)\cdot \mu_j \cdot \Delta t \tag{23}$$

$$\min Z_2 = \frac{1}{S}\sum_{s=1}^{S}\left(\frac{\sum_{t=1}^{T} E_s(t)}{\sum_{t=1}^{T} C_s^{r}(t)} - \frac{1}{S}\sum_{s=1}^{S}\frac{\sum_{t=1}^{T} E_s(t)}{\sum_{t=1}^{T} C_s^{r}(t)}\right)^2 \tag{24}$$

The model aims to minimize the proportion of total lost passenger flow and the variance of average passenger dwell time at all stations of the line. Wan et al. [17] utilized the hybrid genetic particle swarm algorithm and the method of constructing linear weights to tackle the multi-objective model. Taking this as a reference, equation (25) shows the linearly weighted objective functions with weight values ω_1 and ω_2, where $\omega_1 + \omega_2 = 1$.

$$\min Z = \omega_1 Z_1 + \omega_2 Z_2 \tag{25}$$

IV. Algorithm Design

The simulated annealing algorithms are often used to solve non-linear multi-objective planning models. In contrast to ordinary local search algorithms, the simulated annealing algorithm selects states in the neighborhood with relatively low objective values with a fixed probability, making it a globally optimal algorithm in theory. Typically, the initial solution in the simulated annealing process is chosen randomly as a default. However, the initial solution is often chosen randomly by default in standard simulated annealing algorithms. As a result, if the initial solution is a local optimum, applying the simulated annealing algorithm on this basis should yield better results than the random selection of the initial solution. Yane Hou et al. [18] combined the particle swarm algorithm and the genetic algorithm in their study to create a more reliable and efficient calculating algorithm than the standard algorithm. Thus, the solution algorithm adopted in this paper is a hybrid simulated annealing particle swarm optimization algorithm (SA-PSO).

The following describes how to implement the (SA-PSO) algorithm:

Step 1: Initialize the particle swarm's particle positions at random.

Step 2: Evaluate the population and determine each particle's fitness.

Step 3: Particle fitness should be compared to their own pBest optimal value. If the particle's fitness surpasses pBest's fitness, pBest is set to the current position.

Step 4: Compare the particle's fitness to the population's optimum gBest. If the particle's fitness surpasses the gBest's fitness, gBest is set to the current position.

Step 5: Update the position and velocity of the particle according to equation (26).

$$\begin{cases} v_{id}(t+1) = w\times v_{id}(t) + c_1 r_1 \times (P_{id} - x_{id}(t)) + c_2 r_2 \times (P_{gd} - x_{id}(t)) \\ x_{id}(t) = x_{id}(t)\times v_{id}(t+1) \end{cases} \tag{26}$$

Step 6: Verify if the algorithm's convergence requirement is met. If so, end the search for the best. If not, move on to Step 2.

Step 7: Make $T = T_0$, and set the obtained particle positions and their search result values as the initial solution and objective function values.

Step 8: Following the cooling schedule, make T equal to the next value, Ti.

Step 9: Perturb based on the current solution x_i to generate a new solution x_j. Subsequently, the new objective function value $f(x_j)$ is calculated based on the new solution, resulting in $\Delta e = f(x_j) - f(x_i)$.

Step 10: If $\Delta e < 0$, then the solution x_j is taken as the new current solution. If $\Delta e > 0$, then the solution x_j is accepted with probability $e^{-\frac{f(x_j)-f(x_i)}{KT}}$.

Step 11: Perform L_k times of the perturbation and acceptance process at temperature T_i. In other words, perform L_k times of Step 9 and Step 10.

Step 12: Determine whether T has reached T_f. If so, terminate the algorithm. Otherwise, execute Step 8.

Step 13: Output x_j and $f(x_j)$, stop.

V. Example Analysis

A. Basic information

In order to verify the validity of the proposed scheme, the up direction of Shenzhen Urban Mass Transit Line 4 is adopted here as an example for research. The selected line consists of 23 stations (denoted as numbers 1 to 23), as depicted in Fig. 2. To conduct the analysis, the base data utilized is derived from the AFC system data of Shenzhen Urban Mass Transit Line 4 on a certain weekday. The statistical method is employed to collect the required passenger flow information for the model. During the morning peak hours, the passenger flow usually shows a unidirectional pattern. As a result, only the optimization scheme for flow control in the up direction is selected as the research object. Among them, the interchange passenger flow is converted into the passenger flow in and out of the relevant station on the line.

Fig. 3 and Table III show each station's passenger flow and alighting rate during the morning peak from 7:00 to 9:00 a.m. The flow control period has a unit control time granularity of 15 min and a departure interval of 300s.

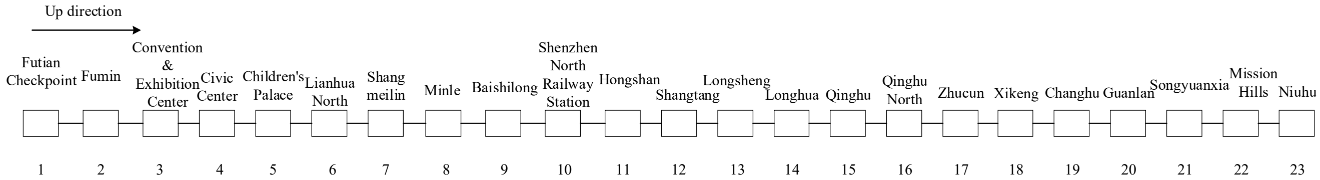

Fig. 2. The distribution of stations on Shenzhen City Rail Transit Line 4

TABLE III
ALIGHTING RATES BY STATION FOR EACH CONTROL PERIOD

Station number	7:00-7:15	7:16-7:30	7:31-7:45	7:46-8:00	8:01-8:15	8:16-8:30	8:31-8:45	8:46-9:00
1	0	0	0	0	0	0	0	0
2	0.03	0.03	0.03	0.04	0.04	0.05	0.05	0.06
3	0.05	0.05	0.04	0.04	0.05	0.05	0.05	0.04
4	0.06	0.06	0.07	0.07	0.08	0.09	0.08	0.08
5	0.18	0.15	0.13	0.13	0.17	0.16	0.18	0.18
6	0.21	0.17	0.17	0.19	0.25	0.27	0.27	0.33
7	0.08	0.08	0.08	0.08	0.08	0.09	0.09	0.08
8	0.19	0.15	0.12	0.1	0.11	0.12	0.15	0.15
9	0.08	0.08	0.07	0.07	0.07	0.08	0.08	0.09
10	0.06	0.06	0.06	0.06	0.06	0.07	0.07	0.07
11	0.09	0.08	0.08	0.07	0.07	0.08	0.08	0.09
12	0.06	0.06	0.06	0.06	0.06	0.07	0.08	0.1
13	0.13	0.14	0.13	0.12	0.11	0.13	0.12	0.13
14	0.11	0.1	0.13	0.13	0.13	0.13	0.12	0.13
15	0.11	0.11	0.13	0.16	0.16	0.17	0.18	0.15
16	0.07	0.08	0.09	0.11	0.14	0.14	0.14	0.14
17	0.17	0.14	0.18	0.19	0.21	0.18	0.19	0.19
18	0.2	0.3	0.35	0.35	0.41	0.36	0.42	0.4
19	0.15	0.18	0.28	0.39	0.56	0.45	0.58	0.49
20	0.23	0.32	0.33	0.32	0.36	0.26	0.3	0.28
21	0.67	0.72	0.55	0.68	0.71	0.55	0.68	0.66
22	0.72	0.75	0.63	0.74	0.76	0.67	0.78	0.71
23	1	1	1	1	1	1	1	1

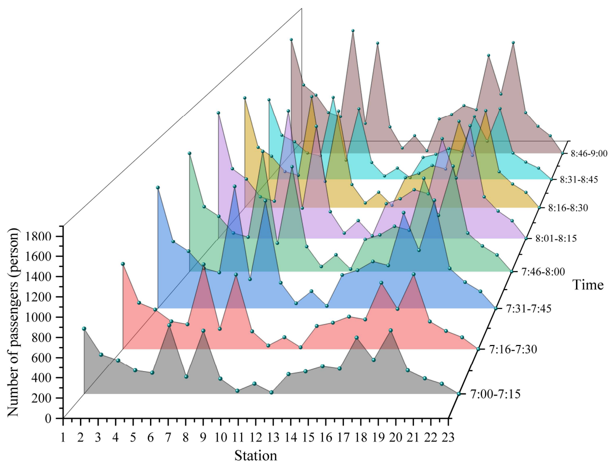

Fig. 3 The distribution of passenger flow by station during each control period

As observed in Fig. 3, the overall passenger flow is high during each control period in the morning peak. Furthermore, it is also evenly distributed at the upstream and downstream stations of the line. These characteristics make it suitable as a data example.

The method of distributing survey questionnaires offline and online was adopted in this study to determine the value of the time perception coefficient parameter. A total of 300 questionnaires were distributed, and 278 questionnaires were recovered, with 249 deemed valid finally. The specific model parameters are shown in Table IV.

TABLE IV
PARAMETERS AND THEIR VALUES

Parameters	Definition	Value
θ	Churn rate	10%
μ_j	Time perception factor	The values are 1, 1.13, and 1.24 for j=1, 2, 3, respectively
ρ	Maximum safe density of passenger flow	4p/m^2
Δt	Control time duration	15min
$\sigma_{\max}$	Maximum full train load ratio	30%
C	Train Capacity	1440 people
S_j	Waiting area effective area	The values are 425m^2, 1000m^2 and 500m^2 for j=1, 2, 3, respectively
ω_1	Weighting factor 1	0.4
ω_2	Weighting factor 2	0.6

TABLE V
PERMITTED TO ENTER THE STATION PASSENGER FLOW CONTROL RATES

Station number	7:00-7:15	7:16-7:30	7:31-7:45	7:46-8:00	8:01-8:15	8:16-8:30	8:31-8:45	8:46-9:00
1	0.23	0.25	0.39	0.08	0.01	0.07	0.16	0.24
2	0.47	0.26	0.50	0.39	0.23	0.26	0.34	0.20
3	0.27	0.41	0.15	0.09	0.33	0.07	0.13	0.30
4	0.39	0.49	0.18	0.32	0.37	0.44	0.13	0.16
5	0.33	0.24	0.42	0.43	0.48	0.46	0.18	0.26
6	0.31	0.25	0.11	0.33	0.43	0.05	0.03	0.08
7	0.44	0.30	0.29	0.22	0.22	0.10	0.28	0.39
8	0.46	0.42	0.21	0.40	0.32	0.16	0.24	0.07
9	0.46	0.26	0.10	0.01	0.27	0.19	0.28	0.34
10	0.28	0.32	0.30	0.15	0.01	0.03	0.02	0.22
11	0.27	0.18	0.21	0.12	0.28	0.21	0.05	0.25
12	0.19	0.29	0.06	0.31	0.29	0.33	0.18	0.18
13	0.16	0.42	0.22	0.17	0.24	0.45	0.37	0.22
14	0.32	0.33	0.11	0.34	0.49	0.24	0.25	0.33
15	0.41	0.38	0.42	0.41	0.48	0.44	0.49	0.11
16	0.16	0.25	0.36	0.47	0.14	0.32	0.40	0.34
17	0.29	0.04	0.14	0.43	0.27	0.11	0.24	0.22
18	0.27	0.28	0.02	0.06	0.23	0.11	0.08	0.21
19	0.25	0.21	0.08	0.02	0.34	0.27	0.26	0.35
20	0.17	0.27	0.43	0.17	0.24	0.23	0.44	0.36
21	0.09	0.29	0.31	0.25	0.37	0.39	0.11	0.02
22	0.28	0.11	0.28	0.38	0.16	0.01	0.24	0.39
23	-	-	-	-	-	-	-	-

TABLE VI
PERMITTED TO ENTER THE PLATFORM PASSENGER FLOW CONTROL RATES

Station number	7:00-7:15	7:16-7:30	7:31-7:45	7:46-8:00	8:01-8:15	8:16-8:30	8:31-8:45	8:46-9:00
1	0.21	0.39	0.38	0.11	0.27	0.35	0.45	0.34
2	0.13	0.39	-	0.42	0.36	0.16	0.21	-
3	0.06	0.22	0.10	0.25	0.42	0.13	0.31	0.20
4	0.42	0.09	0.22	0.26	0.40	0.01	0.03	0.18
5	0.01	0.27	0.01	0.06	-	0.10	0.16	0.16
6	0.44	0.18	0.47	0.29	0.21	0.22	0.33	0.46
7	0.17	0.07	0.33	0.31	-	0.01	0.34	0.36
8	0.04	0.13	0.04	0.38	0.29	0.16	0.37	0.06
9	0.19	0.15	0.14	0.40	0.24	0.23	0.10	0.10
10	0.03	0.46	0.06	0.26	0.18	0.26	0.24	0.24
11	0.26	0.42	0.23	0.29	0.34	0.05	0.04	0.14
12	0.31	0.15	0.32	0.23	0.08	0.10	0.09	0.23
13	0.39	-	0.19	-	0.33	0.24	0.22	0.17
14	0.22	0.01	0.19	0.21	0.07	0.12	0.15	0.21
15	0.09	0.11	0.11	-	0.02	0.01	0.15	0.42
16	0.28	0.21	0.01	0.15	0.27	0.16	0.01	0.10
17	0.46	0.44	0.44	0.39	0.27	0.17	-	0.10
18	0.17	0.34	0.39	0.38	0.28	0.30	0.16	0.10
19	0.25	0.40	0.31	0.26	0.27	0.05	0.36	0.04
20	0.14	0.08	0.11	0.22	0.12	0.13	0.01	0.33
21	0.07	0.12	0.03	0.22	0.18	-	0.26	0.42
22	0.43	0.08	0.23	0.18	0.28	0.32	0.05	0.03
23	-	-	-	-	-	-	-	-

Note: “-” indicates uncontrolled flow

B. Analysis of results

The simulated annealing particle swarm optimization algorithm is designed for model solving. All computational work is done on an intel i3 2.10GHz, 8G RAM, Windows 10 operating system computer, using MATLAB R2016a for solving. After 151.65 seconds of calculation, the algorithm converges in around 200 iterations, resulting in the optimal solution of 1.5246. The results of the optimized flow control scheme are displayed in Tables V and VI.

Based on the information in Tables V and VI, it can be concluded that passenger flow control primarily takes place during the morning rush hour at Shenzhen urban rail line 4 stations 2, 4, 5, 14, 15, 16, and 20. These stations are frequently high-flow stations or located between high-flow stations. Furthermore, it can be observed that the upstream stations have comparatively higher flow control rates than the downstream stations during each control period. This result ensures the rational distribution of transport capacity on the line, guaranteeing fairness in urban rail mass services for passengers.

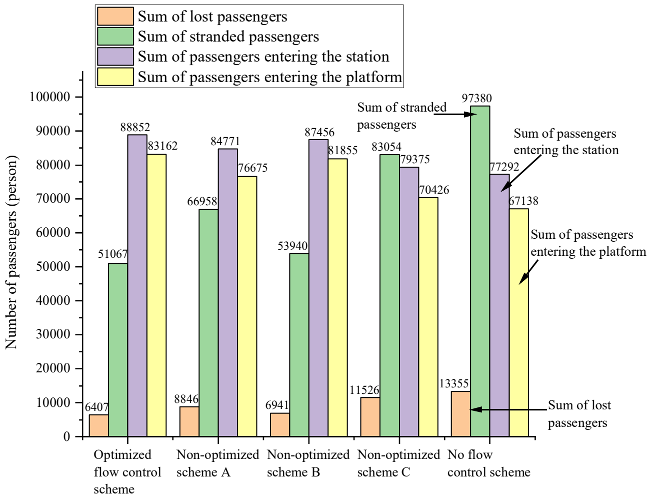

Fig. 4. Indicator values under each flow control scheme

The passenger flow situation under the no flow control and the three types of non-optimized flow control schemes are selected for comparison and reference.

Specifically, the service balance of the stations on the line is not taken into consideration for the non-optimized scheme A. The maximum safe passenger density constraint for each area is not taken into consideration for the non-optimized scheme B. The max flow control factor constraint is not taken into consideration for the non-optimized scenario C. Besides, only the maximum full train load factor is considered for the no flow control scheme.

The results for the three types of optimized flow control, non-optimized flow control, and no flow control schemes are displayed in Fig. 4. The indicators include the sum of lost passengers, the sum of stranded passengers, the sum of passengers entering the station, and the sum of passengers entering the platform.

Compared to the non-optimized scheme A, the optimized flow control scheme effectively reduces the sum of lost and stranded passengers by approximately 27.6% and 23.7%, respectively. Additionally, there is an increase of roughly 4.8% in the sum of passengers entering the station and about 8.5% in the sum of passengers entering the platform.

Compared to the non-optimized scheme B, the optimized flow control scheme effectively reduces the sum of lost passengers and stranded passengers by approximately 7.7% and 5.3%, respectively. Besides, there is an increase of roughly 1.6% in the sum of passengers entering the station and about 1.6% in the sum of passengers entering the platform.

Compared to the non-optimized scheme C, the optimized flow control scheme effectively reduces the sum of lost and stranded passengers by approximately 44.4% and 38.5%, respectively. Furthermore, there is an increase of roughly 11.9% in the sum of passengers entering the station and about 18.1% in the sum of passengers entering the platform.

Compared to the no flow control scheme, the optimized flow control scheme decreases by approximately 52% and 47.6% in the sum of lost and the sum of stranded passengers, respectively. Meanwhile, the sum of passengers entering the station and the sum of passengers entering the station platform have increased by about 15% and 23.9%, respectively.

From these results, it can be seen that more stranded passengers are permitted to enter the station and the platform under the optimized flow control scheme. This leads to a smaller perceived average dwell time for stranded passengers. Ultimately, the optimized flow control scheme effectively reduces the sum of lost passengers.

In conclusion, adopting the optimized flow control scheme is conducive to a notable rise in the sum of passengers entering the station and the sum of passengers entering the platform. Under this scheme, the standard of urban mass transit passenger service will be significantly improved.

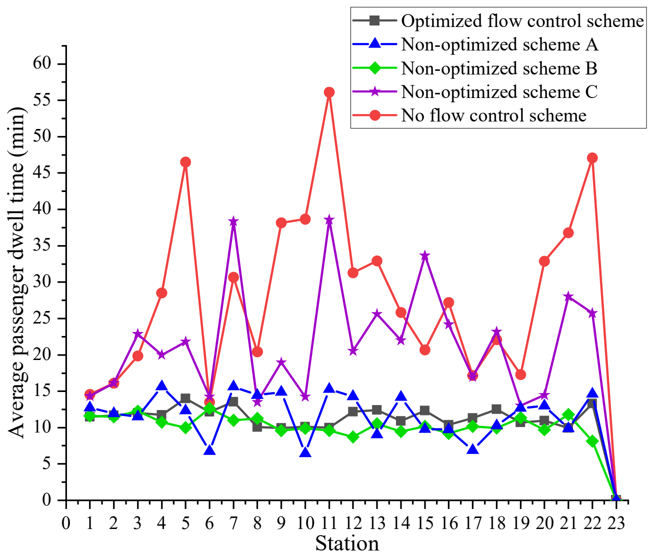

Fig. 5. Average passenger dwell time by station

Fig. 5 shows the average dwell time of passengers at each station under different flow control schemes: no flow control scheme, three types of non-optimized flow control schemes, and optimized flow control scheme. The results demonstrate that under the non-optimized scheme A, stranded passengers experience longer average perceived detention time at stations 4, 7, 8, 9, 11, 12, 14, and 22 than others. This discrepancy suggests a poor fairness in passenger services at these stations.

Moreover, the non-optimized scheme C and the no flow control scheme exhibit a more pronounced fluctuation and higher values in the average detention time of stranded passengers at each station. It suggests that passenger services on the line are overall less equitable under both schemes.

In contrast, the non-optimized scheme B and the optimized flow control scheme achieve a relatively balanced average detention time for stranded passengers at each station. Notably, they significantly decrease the average detention time for passengers at stations 4, 8, 9, 11, 14, and 22.

It demonstrates the effectiveness of the optimized flow control scheme in balancing service equity across the line's stations.

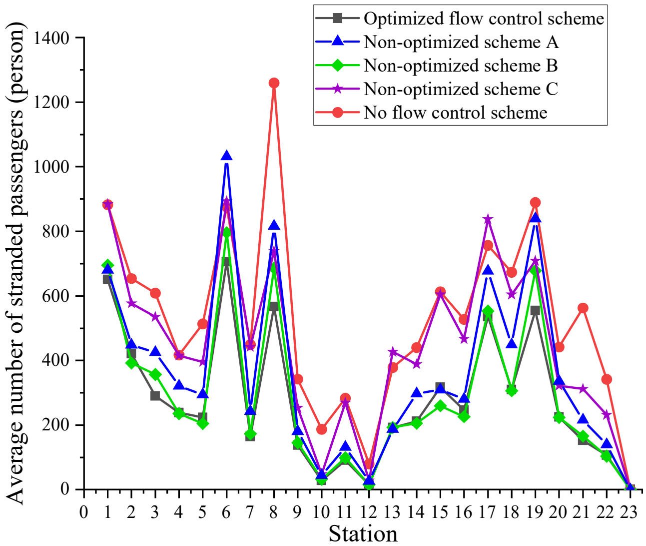

Fig. 6. Average count of stranded passengers by station

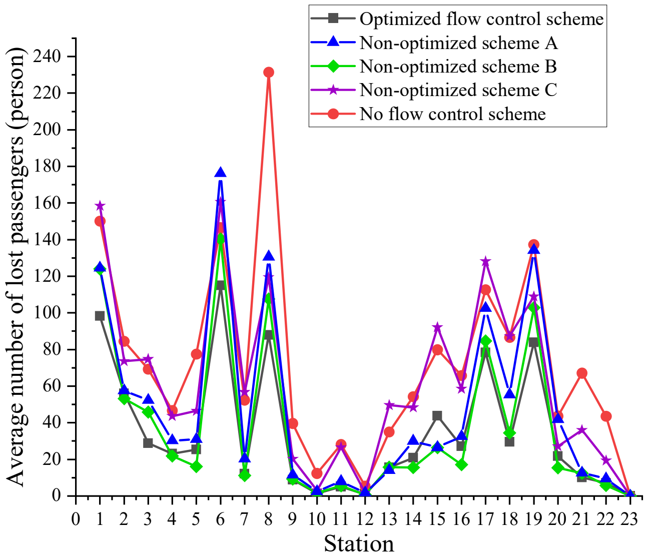

Fig. 7. Average count of lost passengers by station

In the same way, Fig. 6 illustrates the average count of stranded passengers at each station for all schemes. It can be observed that both the optimized flow control scheme and the non-optimized scheme B lead to a smaller average count of stranded passengers at all stations compared to the no flow control and non-optimized schemes A and C. Among them, stations 6, 8, 17, and 19 experienced a significant decrease in the average count of stranded passengers. In particular, the average count of stranded passengers at Station 8 has dropped by 55% under the optimized flow control scheme as opposed to the no flow control scheme.

Furthermore, as shown in Fig. 7, the distribution of the average count of passengers lost at each station under the five schemes follows almost the same trend as Fig. 6. Thus, it can be concluded that the count of stranded passengers exhibits a positive correlation with the count of lost passengers.

All in all, it can be seen that the optimized flow control scheme and the non-optimized scheme B are effective in reducing stranded and lost passengers across the line's stations.

Based on Fig. 8, although the average passenger density in the waiting areas of the station concourse and platform for all periods differ for each station under all five schemes, they fall within the safe range.

Therefore, it can be obtained that there is low potential for passenger congestion in the station concourse and platform waiting areas for all control periods at each station under these five schemes. In other words, urban rail passengers travel with a high degree of safety under these five flow control schemes

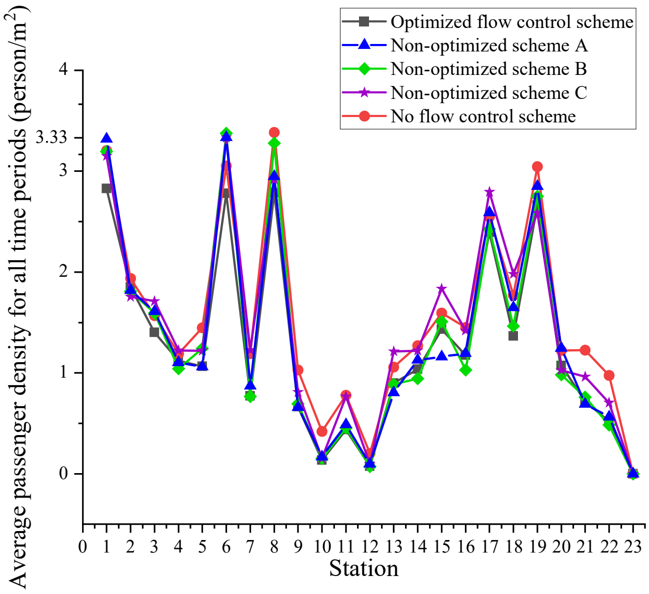

(a) Average outside station passenger density for all periods by station

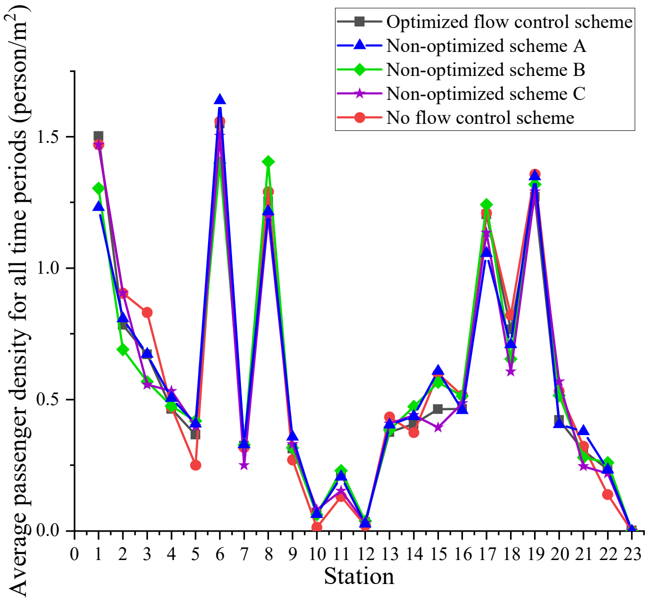

(b) Average density of passengers in the station concourse for all periods by station

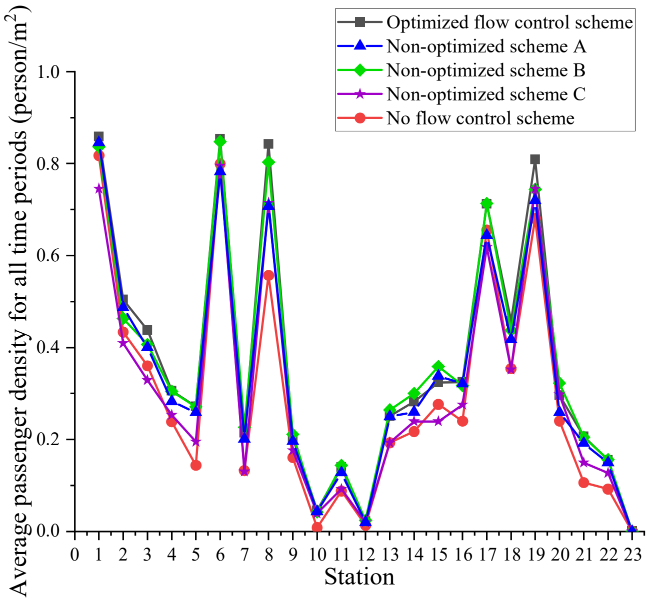

(c) Average density of passengers on the station platform for all periods by station

Fig. 8. Average density of passengers in waiting areas for all periods by station

However, the average passenger flow density exceeds 3.33p/m² in the waiting area outside some stations under the no flow control and non-optimized schemes A and B. It suggests that passengers face more significant safety risks during travel under these three schemes.

On the other hand, the average passenger density in the waiting area outside each station is maintained within 3p/m² when the optimized flow control scheme is employed. Consequently, it can be inferred that implementing the scheme leads to enhanced passenger service safety.

In summary, the optimized flow control scheme balances passenger flow pressure at each station, reducing passenger stay time, the count of lost passengers, and the density of passenger flow. It ultimately improves the fairness and safety of passenger services on the line.

Stations 1, 6, 8, and 19 are the line stations with high passenger flow and effective flow control. As a result, these four stations are selected to compare the passenger densities outside the station under different flow control schemes, as shown in Fig. 9.

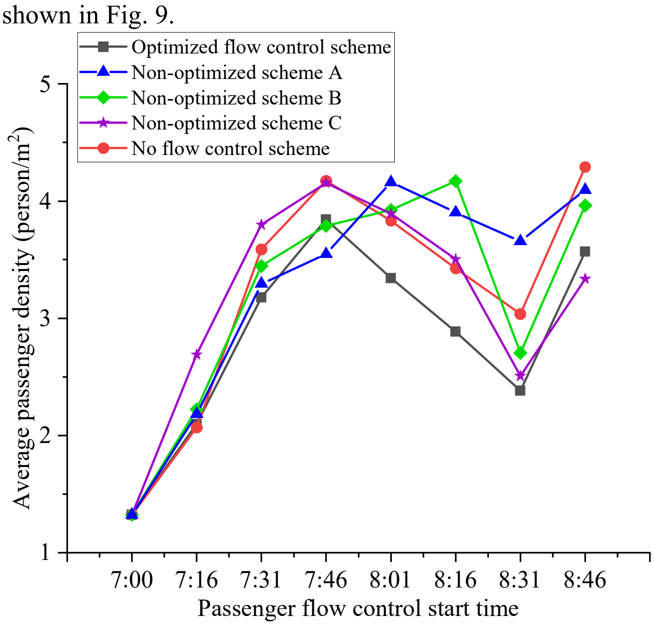

(a) Density of passengers outside Station 1

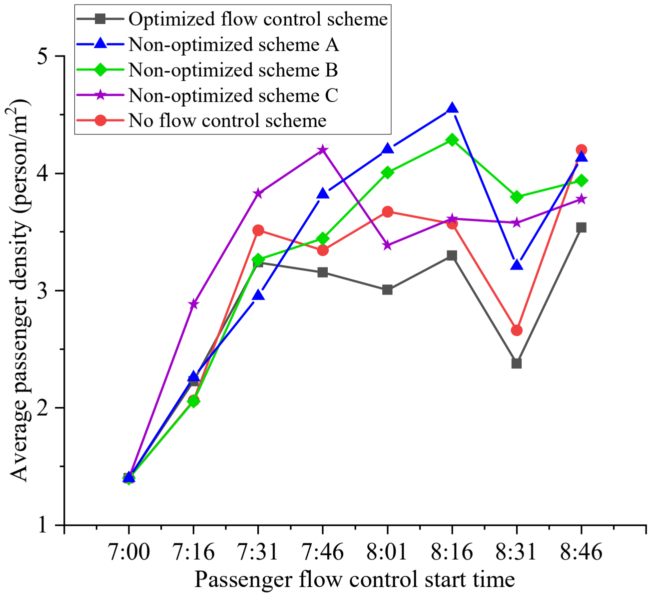

(b) Density of passengers outside Station 6

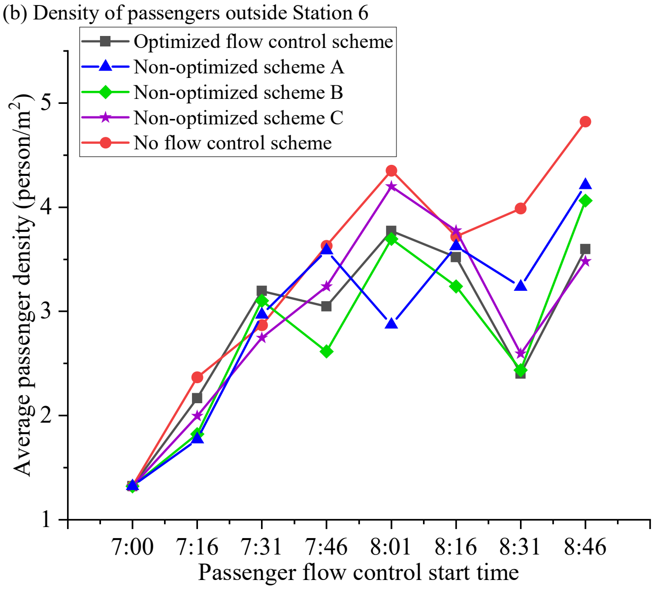

(c) Density of passengers outside Station 8

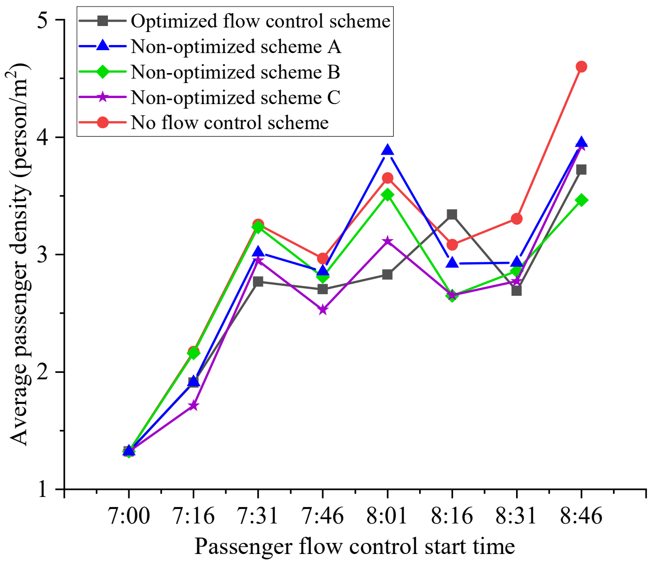

(d) Density of passengers outside Station 19

Fig. 9. Density of passengers in waiting areas outside some stations

According to Fig. 9, under the no flow control scheme and the three types of non-optimized flow control schemes, the density of passengers outside the station exceeds the maximum safe limit at Stations 1, 6, and 8 during some control periods. Besides, the density of passengers outside the station also exceeds the maximum safe limit at Station 19 during some control periods under the no flow control scheme.

Evidently, the overall passenger density in the waiting areas outside Stations 1, 6, 8, and 19 under the other schemes is significantly higher than the passenger density in these waiting areas under the optimized flow control scheme.

This suggests that adopting the other schemes will reduce the safety of passenger travel. Therefore, the optimized flow control scheme is a more reasonable option for ensuring passenger safety.

Similarly, the four stations mentioned above are selected to compare the changes in the count of passengers lost in various waiting areas under different flow control strategies, as shown in Figures 10 and 11.

As seen in Fig. 10, the optimal flow control scheme selection results in fewer lost passengers in the waiting areas outside the four stations, with the count of lost passengers not exceeding 120 in any control period.

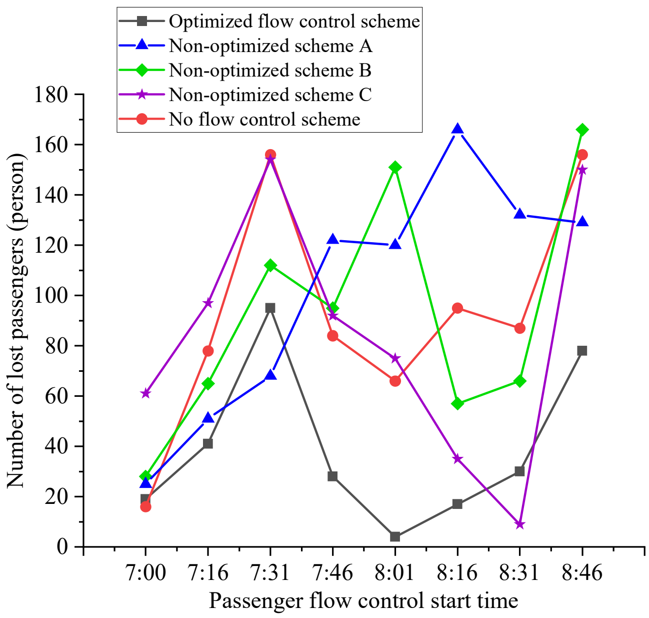

(a) Number of passengers lost outside Station 1

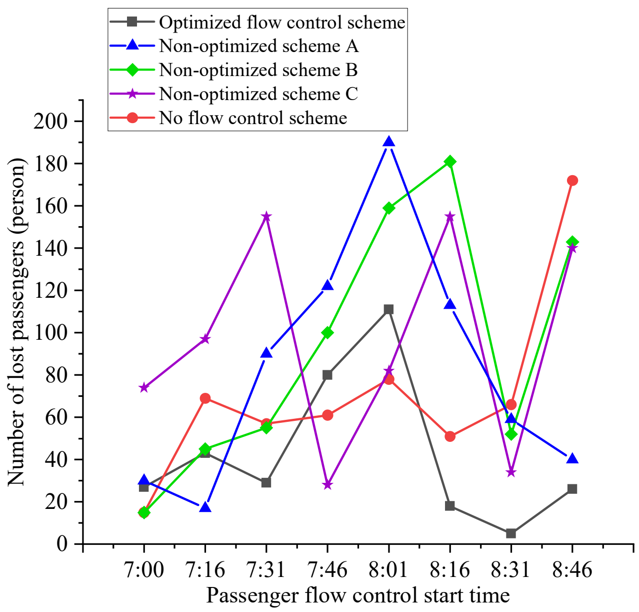

(b) Number of passengers lost outside Station 6

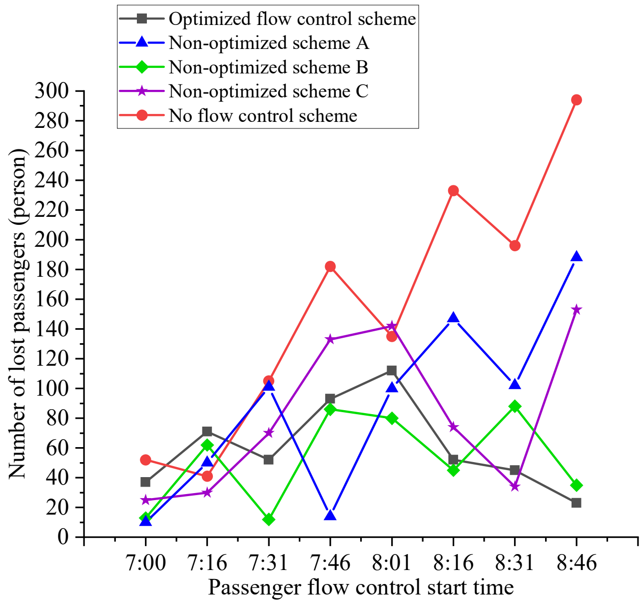

(c) Number of passengers lost outside Station 8

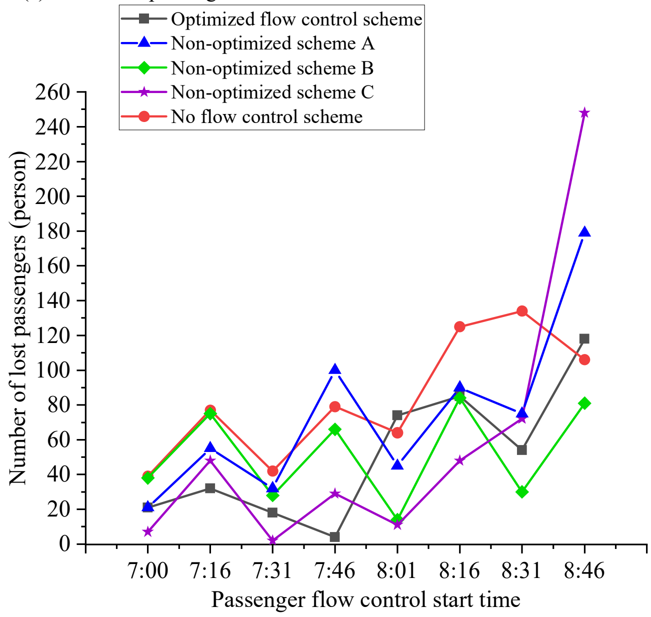

(d) Number of passengers lost outside Station 19

Fig. 10. Number of passengers lost in waiting areas outside some station

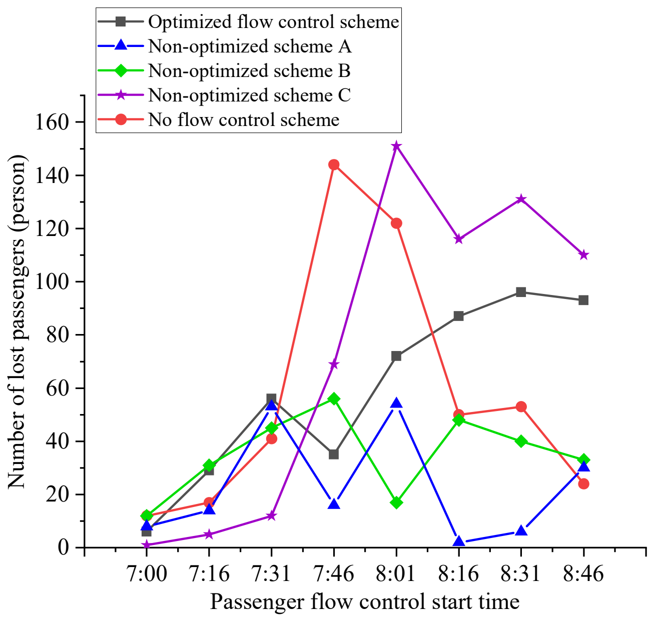

(a) Number of passengers lost in the Station 1 concourse

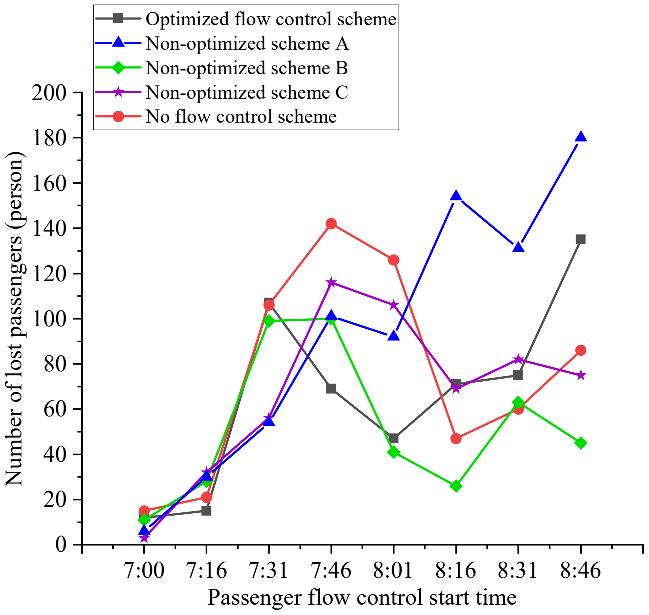

(b) Number of passengers lost in the Station 6 concourse

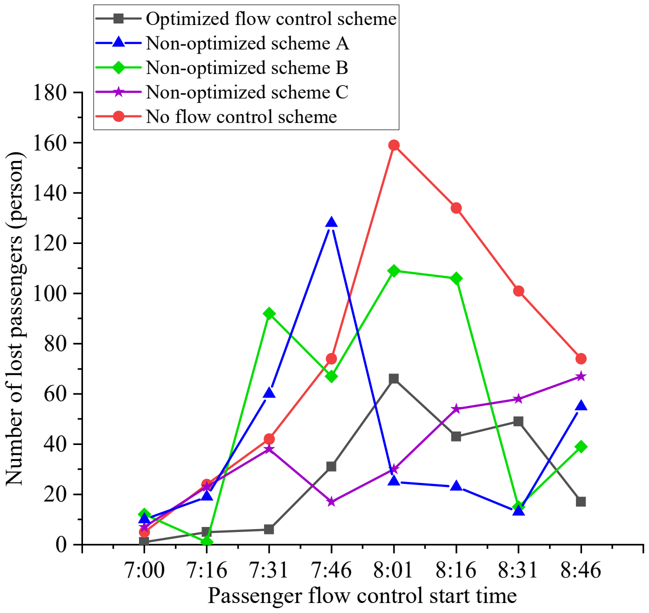

(c) Number of passengers lost in the Station 8 concourse

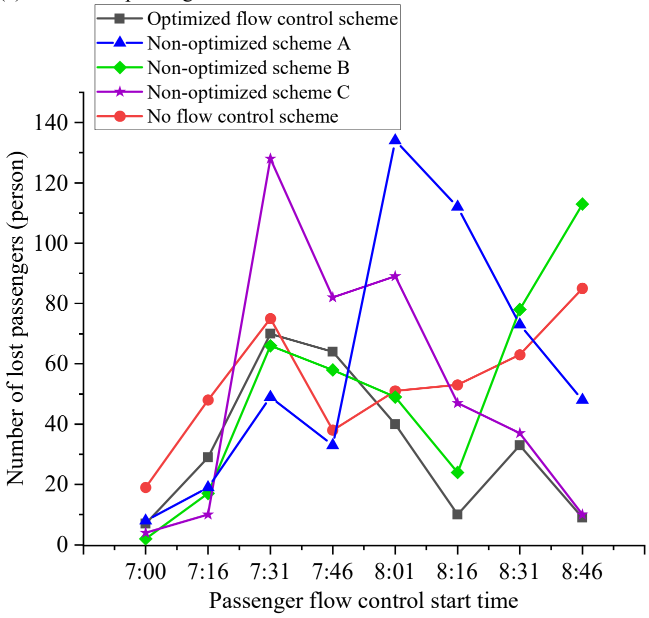

(d) Number of passengers lost in the Station 19 concourse

Fig. 11. Number of passengers lost in the concourse of some stations

As shown in Fig. 11, the optimized flow control scheme for Stations 6, 8, and 19 minimizes passenger loss in the concourse compared to the no flow control scheme and non-optimized schemes A and C. While the optimized flow control scheme leads to more passenger losses in the Station 1 concourse than the non-optimized scheme A, the objective of the model is to minimize overall lost passengers of the line. Besides, while non-optimized scheme B reduces passenger loss in the concourse equally, it does not maintain passenger density within safe boundaries. Therefore, the optimal flow control options are more reasonable from a comprehensive point of view. (comparisons are not made in this paper due to the negligible count of passengers lost at the platform waiting area).

The model deals with two objective functions through the method of linear weighting. Therefore, the value of the weighting factors has an essential impact on the final results. The influence of the correlation between the objective function and the weight coefficient can be seen in Fig. 12.

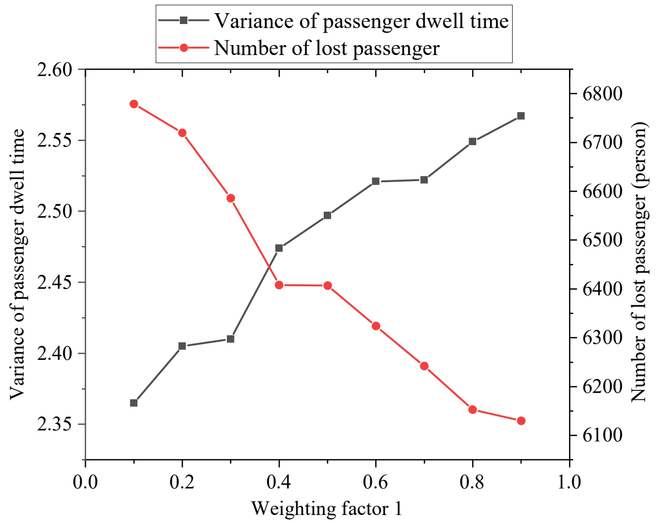

Fig. 12. The correlation between the values of the weighting factor 1 and the objective function

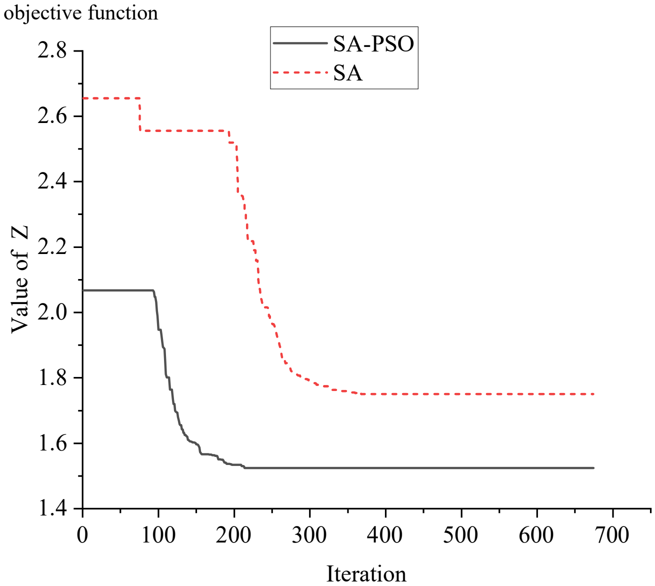

Fig. 13. Convergence process of SA-PSO algorithm and SA algorithm on the objective function

From Fig. 12, the average passenger dwell time variance is positively associated with the value of ω_1, while the sum of lost passengers is negatively connected with the value of ω_1.

When ω_1 is between 0.1 and 0.4, both the rate of decreasing total lost passengers and the rate of increasing average passenger dwell time variance are relatively high. When ω_1 is between 0.5 and 0.8, both the rate of decreasing total lost passengers and the rate of increasing average passenger dwell time variance are relatively low.

To achieve a better dual-objective co-optimization, it takes the value of ω_1 as 0.4 in the paper. This measure will contribute to ensuring the reasonable nature of the final solution to some extent.

Finally, Fig. 13 demonstrates the convergence process of the SA-PSO algorithm. It shows that the SA-PSO algorithm converges faster and better than the traditional SA algorithm. This result validates the effectiveness of the SA-PSO algorithm.

VI. Conclusion

A multi-station passenger flow control scheme for urban rail transit single line considering passenger flow loss is proposed in this paper. A nonlinear multi-objective planning model is developed. The model aims to minimize passenger flow loss proportion and average passenger dwell time variance. The significance of the study is to ensure the service balance, safety, and service efficiency at each station during the morning peak hour. The case study focuses on Shenzhen urban rail transit line 4. The research findings show that:

(1) The hybrid simulated annealing particle swarm algorithm is designed to solve the model. The resulting solution optimizes flow control at all stations of the line during the morning peak hour. According to the result, under the optimized flow control scheme, the reductions in the total count of lost and stranded passengers are approximately 27.6% and 23.7% in comparison to the non-optimized scheme A, respectively. In comparison to the non-optimized scheme B, the reductions are about 7.7% and 5.3%. In comparison to the non-optimized scheme C, the reductions are roughly 44.4% and 38.5%. Meanwhile, compared to the no flow control scheme, the reductions are about 52% and 47.6%, respectively. Furthermore, the sum of passengers entering the station and the sum of passengers entering the platform at each station of the line under the optimized flow control scheme rise by roughly 4.8% and 8.5% in comparison to the non-optimized scheme A, respectively. In comparison to the non-optimized scheme B, these numbers rise by about 1.6%. In comparison to the non-optimized scheme C, these numbers rise about 11.9% and 18.1%, respectively. And these numbers rise about 15% and 23.9% in comparison to the no flow control scheme, respectively.

(2) Under the optimized flow control scheme, the case analysis reveals that the average passenger dwell time and the average count of stranded passengers at each station are smaller and exhibit gentler fluctuations than other schemes. This indicates a reduction in the count of lost passengers in different waiting areas at each station. And it results in a more equitable service to passengers at each station of the line. Besides, the optimized flow control scheme reduces the density of passengers in the various waiting areas, effectively minimizing the risk of gathering passengers. In other words, the optimized flow control scheme decreases the count of passengers congregating at the stations during the control periods to ensure passenger safety.

In conclusion, using the optimal passenger flow control scheme can minimize the sum of lost passengers during peak hours and balance the passenger service of each station on the line. Besides, the scheme improves overall passenger travel safety by reducing passenger density and the risk of overcrowding in various waiting areas. Therefore, the scheme is suitable for urban rail lines with high morning peak passenger flow, clear passenger flow direction, and stable passenger flow status.

References

[1] Jungang Shi, Xiaofang Xiao, Junhua Guo, Hou Dong, "Collaborative passenger flow control model and algorithm for metro with multiple stations in the context of epidemic prevention and control," *China Railway Science*, vol. 44, no. 2, pp. 187-199, 2023.

[2] Zhiya Chen, Jinrong Gan, Xiaojun Wang, "A three-level passenger flow control model for urban mass transit considering safety," *Journal of Central South University* (*Natural Science Edition*), vol. 51, no. 5, pp. 1441-1450, 2020.

[3] Jungang Shi, Lixing Yang, Jing Yang, Feng Zhou, Ziyou Gao, "Cooperative passenger flow control in an oversaturated metro network with operational risk thresholds," *Transportation Research Part C*, vol. 107, pp. 301-336, 2019.

[4] Denghui Li, Qiyuan Peng, Gongyuan Lu, Kun Wang, Zhengyang Wu, "Collaborative passenger flow control method for urban mass transit peak lines," *Transportation System Engineering and Information*, vol. 19, no. 6, pp. 141-147, 2019.

[5] Peng Zhao, Xiangming Yao, Dandan Yu, "Coordinated control of passenger flow in urban mass transit lines during peak hours," *Journal of Tongji University* (*Natural Science Edition*), vol. 42, no. 9, pp. 1340-1346+1443, 2014.

[6] Bin Jia, Ling Zhu, Shukai Li, Jialin Liu, "Collaborative optimization strategy of urban mass transit minor crossing plan and passenger flow control," *Transportation Systems Engineering and Information*, vol. 22, no. 1, pp. 124-132, 2022.

[7] Housheng Zhou, Jianguo Qi, Lixing Yang, Jungang Shi, Congcong Gong, "Research on flexible grouping-based undercarriage utilization plan and robust passenger flow control strategy for urban rail," *Control and Decision*, vol. 38, no. 9, pp. 2663-2671, 2023.

[8] Yahan Lu, Lixing Yang, Fanting Meng, Dongyang Xia, Jianguo Qi, "Collaborative optimization of train schedules and station passenger flow control for urban rail lines," *Transportation Systems Engineering and Information*, vol. 21, no. 6, pp. 195-202, 2021.

[9] Yuan Fuya, Sun Huijun, Kang Liujiang, Lv Ying, Yang Xin, Wei Yun, "An integrated optimization approach for passenger flow control strategy and metro train scheduling considering skip stop patterns in special situations," *Applied Mathematical Modelling*, vol. 118, pp. 412-436, 2023.

[10] Jiajie Li, Yun Bai, Tianjian He, Wenzheng Jia, Tang Li, "Collaborative optimization of train operation planning and passenger flow control on an oversaturated suburban line," *Journal of Central South University*, vol. 30, no. 2, pp. 625-641, 2023.

[11] Jiajie Li, Yun Bai, Yuhe Zhou, Zhijie Chen, Qi Xu, "Collaborative control of large passenger flows in metro interchange stations based on out-of-station flow restriction and schedule adjustment," *Journal of Railways*, vol. 42, no. 5, pp. 9-18, 2020.

[12] Xiangming Yao, Peng Zhao, Ke Qiao, Wenkai Zhang, "Robust optimization model for peak passenger flow control scheme of urban rail lines," *Journal of Railways*, vol. 43, no. 11, pp. 29-37, 2021.

[13] Liang Jinpeng, Zang Guangzhi, Liu Haitao, Zheng Jianfeng, Gao Ziyou, "Reducing passenger waiting time in oversaturated metro lines with passenger flow control policy," *Omega*, vol. 117, 2023

[14] Lu Yahan, Yang Lixing, Yang Hai, Zhou Housheng, Gao Ziyou, "Robust collaborative passenger flow control on a congested metro line: A joint optimization with train timetabling," *Transportation Research Part B*, vol. 168, pp. 27-55, 2023.

[15] Qiwei Jiang, Jiankai Su, Weiya Chen, "Collaborative passenger flow control model for metro considering interstation parking," *Journal of Railway Science and Engineering*, vol. 18, no. 11, pp. 2857-2864, 2021.

[16] Qiuyu Chen, "Research on collaborative flow restriction of urban mass transit oriented to service level equalization," Beijing Jiaotong University, 2021.

[17] Yanchun Wan, Shudi Wang, Yujun Hu, Yanyang Xie, “Multiobjective Optimization of the Storage Location Allocation of a Retail E-commerce Picking Zone in a Picker-to-parts Warehouse,” *Engineering Letters*, vol. 31, no. 02, pp. 481-493, 2023.

[18] Yane Hou, Chunxiao Wang, Weichuan Dong, Lanxue Dang, “An Improved Particle Swarm Optimization Algorithm for the Distribution of Fresh Products,” *Engineering Letters*, vol. 31, no. 02, pp. 494-503, 2023.